Excitation Energy Dependent Efficiency of Charge Carrier Relaxation and Photoluminescence in Colloidal InP Quantum Dots

Randy J. Ellingson,* Jeff L. Blackburn, Pingrong Yu, Garry Rumbles, Olga I. Mićić, and Arthur J. Nozik

Center for Basic Science, National Renewable Energy Laboratory, Golden, Colorado 80401

Received: February 20, 2002; In Final Form: May 13, 2002

Femtosecond transient absorption spectroscopy has been used together with time-integrated photoluminescence (PL) measurements to study charge carrier relaxation in colloidal InP quantum dots (QDs). Measurements of band-edge photoinduced bleaching as well as PL intensity measurements indicate that the fraction of charge carriers relaxing to the band-edge states depends on excitation wavelength, with a markedly reduced relaxation efficiency observed for excitation well above the absorption edge. The results concur with previous research on CdSe and InP QDs, and suggest that with increasing excitation energy there arise relaxation pathways involving surface or external energy states exhibiting reduced radiative efficiency. Such highly excited carriers are either inhibited or deviated from reaching the band-edge states. Excitation intensity dependent measurements indicate that those charge carriers which contribute to the band-edge absorption bleaching also contribute proportionally to the time-integrated PL spectrum.

Introduction

Colloidal nanocrystalline semiconductor quantum dots (QDs) exhibit discrete atomic-like energy levels, and optical properties which depend critically on both particle size and the particle surface chemistry. The sub-100-Å particle sizes accessible by colloidal synthesis techniques provide a unique opportunity to study the electronic and optical properties of strongly quantum confined charge carriers. While considerable research has been reported on the optical spectroscopy of photoexcited charge carriers in nanocrystalline II−VI materials such as CdSe and CdS, there have been few reports on III−V nanocrystals such as InP and InAs. Colloidal nanocrystals from these two classes share many properties, including a confinement-induced shift of the band edge to higher energies and emission properties strongly influenced by the surface treatment of the particles. The absorption spectrum of a colloidal solution containing a distribution of InP QD sizes shows an exciton absorption shoulder or peak at the first exciton energy, followed by one or two additional features attributed to higher energy excitonic transitions. As prepared, InP QDs are capped with the organic surfactant molecules trioctylphosphine oxide (TOPO) and trioctylphosphine (TOP). Photoexcitation of TOPO/TOP capped InP QDs results in weak band gap emission peaking at an energy slightly below the first exciton absorption feature, with deep trap emission prominent at lower energies.[1] Substitution of the TOPO/TOP with pyridine quenches photoluminescence (PL) altogether; in contrast, etching the as-prepared particles using a dilute solution of hydrogen fluoride can improve the PL quantum yield (QY) to as high as 30% at room temperature.

Previous research has shown that CdSe and InP colloidal QDs exhibit a luminescence QY which decreases for higher excitation photon energies.[2−4] In particular, Hoheisel et al.[2] published results of low-temperature luminescence excitation studies in which 32 Å diameter CdSe QDs dots indicated absorption into a quasicontinuum of levels for excitation energies greater than ∼300 meV above the first transition, as evidenced by a drop in PL. Rumbles et al.[3] published photoluminescence excitation studies of colloidal InP QDs showing a dramatic departure of the PL QY from the shape of the absorption spectrum. While the nature of the observed PL QY anomaly has yet to be pinpointed, possible explanations introduced by the authors included a photoionization threshold or excitation into states associated specifically with the nanoparticle surface.[2] Quantum dots prepared by colloidal methods have a large number of surface atoms. Bonds involving surface atoms are frequently unpassivated, and are known to act as trapping centers for charge carriers. Our investigation of the excitation wavelength dependence of both normalized band-edge bleaching and time-integrated PL of InP QDs also indicates that photoexcitation into higher lying energy levels results in significantly reduced efficiency of charge carrier relaxation to the band edge.

Experimental Section

Indium phosphide QDs were synthesized by standard colloidal methods as previously reported,[5] starting by heating a mixture of indium oxalate, tris(trimethyl)phosphine, and a 0.1:1 ratio of trioctylphosphine oxide (TOPO) and trioctylphosphine (TOP). The zinc blende InP nanocrystals measured here have a mean diameter of 42 Å, with a size distribution of $\sim \pm 10\%$. The TOPO/TOP organic capping groups serve to stabilize the dots against oxidation while also solubilizing them for suspension in organic solvents such as hexane and toluene. The TOPO/TOP organic capping groups effect the partial passivation of surface dangling bonds. However, band-edge luminescence generally remains weak (quantum yield of ∼1%) unless the QDs are etched. Similar to previous reports which employed an alcoholic solution, we etch the particles using a dilute methanolic solution of HF or NH_4F, in the presence of TOPO/TOP.[5] Etching increases the near-band-edge photoluminescence by a factor of 10 or more, and reduces the near-infrared emission indicative of deep surface trap states.

Transient absorption (TA) measurements are conducted on colloidal QD solutions in hexane, contained in fused silica

10.1021/jp025666p CCC: $22.00
Published on Web 07/20/2002

cuvettes of 1 mm or 2 mm path length. Our TA setup is based on a Clark-MXR CPA-2001 regeneratively amplified Ti: sapphire laser, operating at 989 Hz. The 775 nm output pulses pump an optical parametric amplifier (OPA), providing output tunable in the visible. We use β-$BaBO_4$ (BBO) to frequency double a fraction of the 775 nm beam to generate 387 nm pulses; focusing a few milliwatts of Ti:sapphire output onto a 2 mm sapphire window generates probe pulses of white light (WL) continuum which range from ~440 nm to 950 nm. Probe pulses are delayed relative to the pump using an optical delay line capable of up to 300 ps delay.

Calculation of the excitation density requires knowledge of the concentration of nanoparticles in solution, which we determine from the decadic extinction coefficient ϵ using $c = \mathrm{OD}/(d\epsilon)$, where OD is the sample optical density at the pump wavelength, d is the sample thickness, and c is the molar concentration of QD particles. The absorption cross section $\sigma_a = -\ln(T)/(dc)$ is then used to calculate the average excitation density per particle, $\langle N_0 \rangle$, using the product of the pump fluence (photons per pulse per cm^2) and the absorption cross section, $\langle N_0 \rangle = j_p \sigma_a$. The extinction coefficient for InP QDs, $\epsilon = (4.2 \pm 0.4) \times 10^5\ cm^{-1}\ M^{-1}$, has been determined for InP QDs using classical chemical methods by measuring the optical absorption for known monomer concentration and particle size. The sample OD was 0.6 for the highest excitation energy (3.2 eV) and 0.1 for the lowest excitation energy (2.0 eV). Measurements are made over a range of excitation densities, from 0.5 to ~2 excitons per dot; exciting at 0.5 electron−hole pair per dot simplifies experimental interpretation by avoiding multipair Auger recombination effects.[6] Measurements of the pump pulse transmission as a function of pump intensity reveal a slight self-bleaching (ranging up to ~5%−8% for $\langle N_0 \rangle = 4$) during the pulse which must be accounted for in exciton density calculations.

Accurate assessment of the band-edge transient bleaching dependence on excitation wavelength requires careful measurement of the pump beam intensity. The spatial beam profiles of both the 387 nm frequency-doubled Ti:sapphire and the OPA signal beam exhibit considerable higher order non-TEM_{00} modes. We therefore spatially filter the beam, using focusing and collimating lenses of 100 mm focal length and a 25 μm pinhole near the beam focus. Transmission of the spatially filtered beam through a nonaperturing iris blocks higher order radially diffracted light, and the resulting output beam has an approximately Gaussian profile. The pump and probe pulses are focused to spot sizes of 420 and 125 μm, respectively. The pump beam is chopped using a New Focus Model 3501 phase-locked chopper which is synchronized to the pulse train using the output from the CPA-2001 controller (DT505). Proper adjustment of the chopper phase allows every other pulse of the pump beam to be blocked. The probe pulses, which are dispersed using a CVI DK240 0.25 m monochromator, are detected using a silicon detector and digitized by a Stanford Research SR250 integrated averager. Comparison of the probe intensity with and without the pump permits calculation of the differential transmission, $\Delta T/T_0$, which can in turn be converted to differential absorption, $\Delta\alpha/\alpha_0$, using the linear absorption of the sample at the probe wavelength. We measure the differential absorption either as a function of probe wavelength at a fixed delay or as a function of delay at a fixed probe wavelength. Correction for chirp is accomplished using a 0.5 mm ZnO crystal to determine the two-photon absorption correlation peak dependence as a function of time, and then using a lookup table to set the physical delay to accommodate the chirp at each specific probe wavelength.[7]

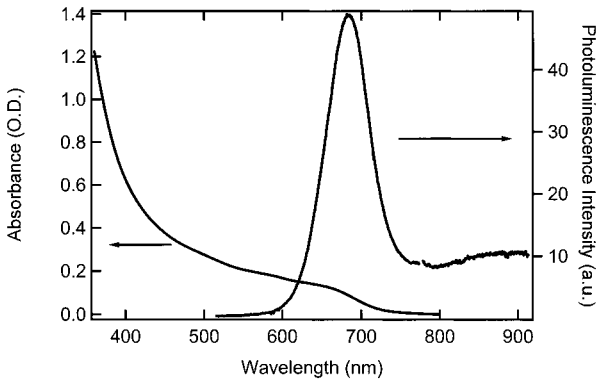

Figure 1. Absorption and global photoluminescence spectra for a suspension of TOP- and TOPO-capped InP QDs in hexane with a mean diameter of 42 Å. The sample was excited at 3.20 eV for the photoluminescence measurement. Emission beyond about 775 nm is attributed to deep trap luminescence.

Steady-state absorption measurements were made using a Cary 500 double beam spectrometer at a spectral resolution of 1 nm. Time-integrated PL spectra resulting from the OPA pump source were recorded by collecting and focusing emission onto a fiber bundle light guide coupled into a Triax 190 spectrometer with CCD detection system. Our TA experimental arrangement allows measurement of the time-integrated PL immediately after the transient bleaching measurement, with no change to either the sample position or excitation beam. At each excitation wavelength, we adjust the focusing of the spatially filtered beam to produce a 420 μm diameter excitation spot size. By adjusting the excitation spot size to be constant and adjusting the pulse energy according to the linear absorption, we equalize the total number of photons absorbed for each excitation wavelength. We align for overlap of pump and probe using a 150 μm diameter pinhole, and we block the WL probe to record the PL spectrum. When collecting PL for 387 nm excitation, we filter scattered excitation light using a Schott GG435 color glass filter. To filter scattered pump light from PL spectra collected for other excitation wavelengths, we use crossed polarizers (Newport Corporation, 10LP-VIS) before and after the sample. All spectra have been corrected for collection and detection sensitivity response. All spectroscopic measurements were conducted at room temperature.

Results

We have measured the time-integrated PL and the first-exciton transient bleach signal for InP QDs at four different excitation energies. Our results indicate that the efficiency with which charge carriers relax to the band-edge states decreases with increasing excitation photon energy. Figure 1 shows linear absorbance and global PL emission (i.e., emission from all particles) for our colloidal sample of etched 42 Å diameter InP QDs. The global PL was recorded using 989 Hz excitation at 387 nm, for an average per-dot initial exciton density of 0.5. The width of the PL spectrum is dominated by inhomogeneous broadening due to the $\sim \pm 10\%$ size distribution. While PL at energies far to the blue of the PL peak is attributed to small particle emission and perhaps also to upconversion of relaxed excitons,[8] we attribute low-energy PL beyond ~775 nm to deep trap state emission. The global PL shows an ~80 meV Stokes shift from the first exciton absorption.

Figure 2 shows corrected time-integrated PL spectra, for four excitation energies ranging from 2.00 to 3.20 eV. Spectra

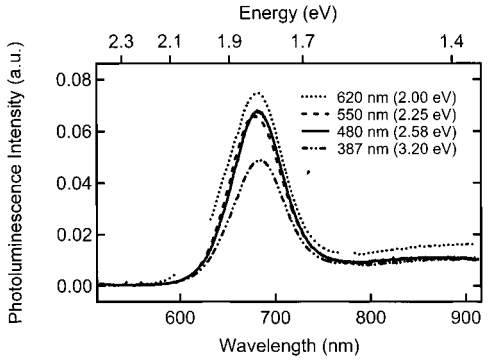

Figure 2. Indium phosphide quantum dot time-integrated photoluminescence spectra resulting from excitation at four different excitation energies. In each case, the pump intensity was chosen to excite an average of $\langle N_0 \rangle = 0.5$ exciton per nanoparticle.

represent the average of two separate sets of measurements on the same etched sample. The photoluminescence spectra, resulting from excitation to an average per-dot exciton density of 0.5, vary depending upon the excitation wavelength. In particular, whereas the spectra for 2.58 and 2.25 eV excitation are of comparable magnitude, the 3.20 eV spectrum shows a reduced PL yield; in contrast, the emission from 2.00 eV excitation shows the best PL yield. Emission at the PL peak of ~684 nm (1.81 eV) is reduced by ~35% when exciting at 3.20 eV as compared to 2.00 eV excitation. Although the spectra for excitation at 2.58 and 2.25 eV are not dissimilar, the four spectra together show agreement with earlier results of photoluminescence excitation studies of InP QDs.[3] These results are also in agreement with the observations of W. Hoheisel et al. studying PL efficiency in CdSe QDs,[2] and indicate an alternate nonradiative relaxation channel becoming available to excitons with sufficient initial energy.

We believe that the time-integrated PL consists of radiative recombination from charge carriers which have cooled to the band edge, and that very little emission results from hot excitons. The broadening of the PL spectra results from inhomogeneous broadening due to the finite size distribution. The time-integrated PL spectra cannot, alone, provide complete information on the efficiency with which electrons and holes relax back to the band edge. Because of this, we used ultrafast TA to provide an independent measure of the time-dependent populations of charge carriers at their respective band edges. Energy level occupation, also known as state-filling, bleaches the absorption of the occupied transitions. Due to the hole's larger effective mass and the concomitant closely spaced energy levels near the valence band (VB) edge, the hole may occupy one of many different VB levels. Based on the relative energy spacings of the conduction band (CB) and VB levels, electrons are expected to dominate both the dynamics and spectral dependence of the TA signal. Further consideration of the contributions of electrons and holes to the TA signal will be presented in the Discussion section. We determine the first exciton absorption energy using the peak of the TA spectrum measured at a delay of ~10 ps, a delay sufficient to ensure the sample is not undergoing initial electronic relaxation which may slightly alter the position of the lowest energy interband transition.

The sample we studied showed a maximum bleaching signal at 1.91 eV; this energy we correlate to the lowest allowed exciton absorption transition (referred to as the 1S exciton transition), or so-called band edge. Measuring the photoinduced bleaching at the band-edge energy as a function of pump wavelength allows us to observe the dynamics of charge carrier relaxation to the band edge. Figure 3 shows TA dynamics,

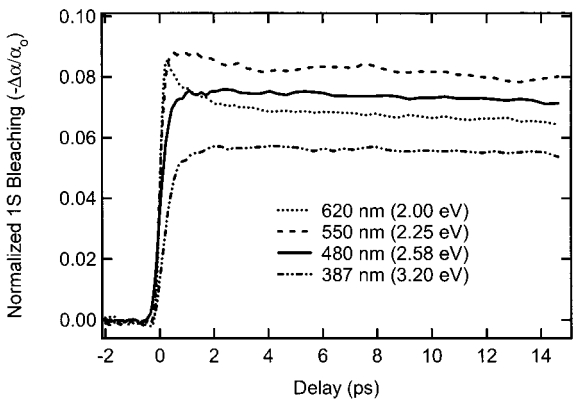

Figure 3. Transient absorption dynamics showing the 1S bleaching intensity of InP quantum dots for four different excitation energies at $\langle N_0 \rangle = 0.5$.

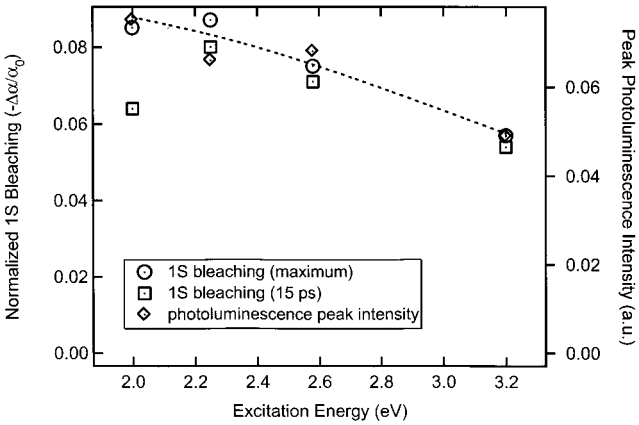

Figure 4. Band-edge photoinduced bleaching and photoluminescence response as a function of excitation energy. The dashed line serves as a guide to the eye.

measured at 1.91 eV, for four different excitation energies, 2.00, 2.25, 2.58, and 3.20 eV. We ascribe the dynamics of the rise time to charge carrier cooling; higher energy excitons require additional time to cool to the band edge. Since we excite to an average concentration of 0.5 exciton per dot, multiple-exciton dynamics do not affect the bleaching data. Pumping at 3.20 eV results in the smallest band-edge bleaching signal, indicative of a relatively inefficient return of charge carriers to the band-edge states. Data for excitation at 2.58 and 2.25 eV show an increasingly efficient relaxation with decreasing excitation energy. TA data for 2.00 eV excitation shows a very fast rise of the bleach to approximately the same level as for the 2.25 eV excitation, but then drops with a ~1.3 ps time constant to a bleaching level lower than the 2.58 eV data. Pumping the sample at 2.00 eV results in slight size selection since for a small fraction (~5%) of the dots the first exciton absorption lies below 2.00 eV. However, for the particles which are excited, the per-dot excitation level still lies close to 0.5 exciton per dot. For excitation energies above the 1S but below the 1P exciton transition (~1.91−2.26 eV), the photon energy is not sufficient to populate the $1P_e$ CB level. For 2.00 eV photon energy, then, the excitonic transition results in the hole receiving ~90 meV of "excess" energy above the first VB level. Since the electron instantaneously occupies the $1S_e$ level and cannot impart energy to the hole, we believe the 1.3 ps relaxation feature reveals a hole relaxation process between VB states near the band edge.

Figure 4 presents a comparison of TA and PL peak data for the four excitation energies. Two sets of TA data are shown,

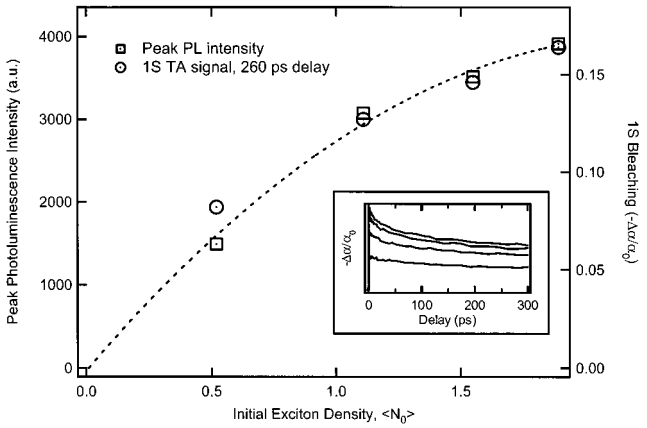

Figure 5. Intensity-dependent band-edge photoinduced bleaching and photoluminescence values as a function of photoexcited exciton density. The excitation energy is 3.20 eV. The dashed line serves as a guide to the eye. Inset shows the individual transient absorption dynamics data for each of four excitation densities.

one for the case of maximum bleaching and the other corresponding to the bleach at 15 ps delay, at which time the initial excitation-energy-dependent relaxation dynamics are complete. Apart from the 2.00 eV data, the TA data for 15 ps delay and for maximum bleach show a monotonic increase in charge carrier relaxation efficiency as the excitation energy decreases; the PL intensity data follow a similar trend. The TA and PL data in large part concur, and they indicate that those charge carriers which arrive at their respective band edges, as evidenced by the TA data, have an equal propensity for radiative recombination independent of initial excitation energy. Photoluminescence lifetimes are typically on the order of ~10 ns for 300 K; TA data on this sample indicate a carrier lifetime in the range of nanoseconds. Since the emission detected by our time-integrated PL measurement occurs over a relatively long time scale, we expect the relationship between PL intensity and 1S bleaching to better match for the 15 ps delay than for the TA bleach maximum. While additional measurements may clarify the data, the TA data point at 2.00 eV, 15 ps delay may represent an anomaly, for which we currently do not have an explanation.

We have measured the excitation intensity dependence of PL and 1S TA for 3.20 eV pump energy, for $\langle N_0 \rangle$ values ranging from 0.5 to 1.9 (see Figure 5). Although not presented here, our measurements show a smaller saturation level for the absorption change versus exciton density for InP QDs than has been reported for CdSe QDs.[6] One expects that the 1S exciton absorption should nearly completely saturate at the level of $\langle N_0 \rangle = 2$; we observe a value for $\Delta\alpha/\alpha_0$ substantially less than 1 at $\langle N_0 \rangle \approx 2$, the explanation for which remains open. We note here, however, that an incomplete 1S bleaching is consistent with the anomalous energy-dependent relaxation efficiency discussed above. Further, we do observe an excitation-energy-dependent 1S bleaching saturation value at high $\langle N_0 \rangle$, with a measurably larger $\Delta\alpha/\alpha_0$ when exciting nearer the first exciton absorption (for example, for $\langle N_0 \rangle \approx 10$, the 1S exciton $\Delta\alpha/\alpha_0$ saturates at ~0.4 for 2.7 eV excitation and at ~0.6 for 2.05 eV excitation). The absorption bleach data in Figure 5 intrinsically pass through the point (0,0); above about $\langle N_0 \rangle = 0.5$, the absorption change becomes nonlinear. Following excitation at multiple-exciton levels, Auger recombination follows on a time scale dependent upon the exciton density. The two-exciton lifetime we measure for 42 Å InP QDs is 55 ps. When excess excitons have recombined so that one pair remains within the dot, the dynamics of recombination resume the "normal" behavior corresponding to the nanosecond-scale charge carrier lifetime. Thus, while the short-time (~1 ps) photoinduced bleaching is not expected to correlate well with the intensity of time-integrated PL, we expect the bleaching observed at longer delays to correlate well with the time-integrated PL intensity. As shown in Figure 5, the PL peak intensity and the 1S bleach at 260 ps delay deviate from linear in a similar manner. Therefore, the data support the conclusion that charge carriers which contribute to the 1S bleach signal at 260 ps delay contribute with equal propensity to the time-integrated PL intensity.

Discussion

Photoluminescence and transient absorption measurements have shown that electronic relaxation in InP QDs proceeds with decreasing efficiency as the excitation photon energy increases (see Figures 2−4). The relaxation channel followed by the excitons lost from the first exciton bleaching and the time-integrated PL is not known. Important questions raised by the effect include the following. Are electrons, holes, or both responsible for the reduced relaxation efficiency? What role do surface states and/or capping molecules play in the relaxation efficiency? How is the excitonic energy distributed, at the moment of excitation, between the electron and the hole? To approach these questions, we must first understand the essential features of QD excitonic absorption, and how this absorption differs from the bulk picture.

When a bulk semiconductor absorbs a supra-band-gap photon, the electron and hole generated share the excess energy such that total momentum is conserved. Owing to the ratio of the electron and hole effective masses in InP ($m_{hh}^*/m_e^* \sim 8$), momentum conservation requires for bulk InP that the electron receives ~8 times more kinetic energy than does the hole. In contrast to the bulk, momentum conservation must be treated differently for QDs. In QDs a third particle is not required in addition to the electron (or hole) and photon in the absorption event to satisfy momentum conservation. Here the QD boundaries play the role of the "third particle" since they provide the required momentum exchange in the (electron/hole) scattering event involving them. This leads to relaxation of conservation of total momentum. For example, in model QDs of perfect spherical symmetry having an infinite surface energy barrier, only angular momentum must be conserved for most kinds of excitations. More complicated, but still relaxed, momentum conservation laws will hold for real-world QDs.

The QDs in our particular sample have a small mean diameter (42 Å), and therefore offer the possibility for interband transitions which do not satisfy conservation of total momentum. In fact, varying the excitation energy likely leads to transitions in which the charge carrier (electron or hole) receiving the majority of excess energy above the first exciton energy depends on specific excitonic resonances. Interband transitions induced by absorption of photons with considerable excess energy are difficult to address theoretically, owing to computational demands which increase rapidly far from the band edge. The majority of current models do not or cannot address high-energy excitations. Also, in almost all models the surface is poorly described, which prohibits analysis of the momentum exchange in the electron (or hole) scattering event with the surface. In particular, the magnitude of the momentum changes are not well described. Further, surface related relaxation pathways lie beyond the reach of most popular models. Thus, we believe the experimental results herein may offer new challenges to theory.

There are two primary contributions to the absorption change induced by absorption of a supra-band-gap photon: the carrier-

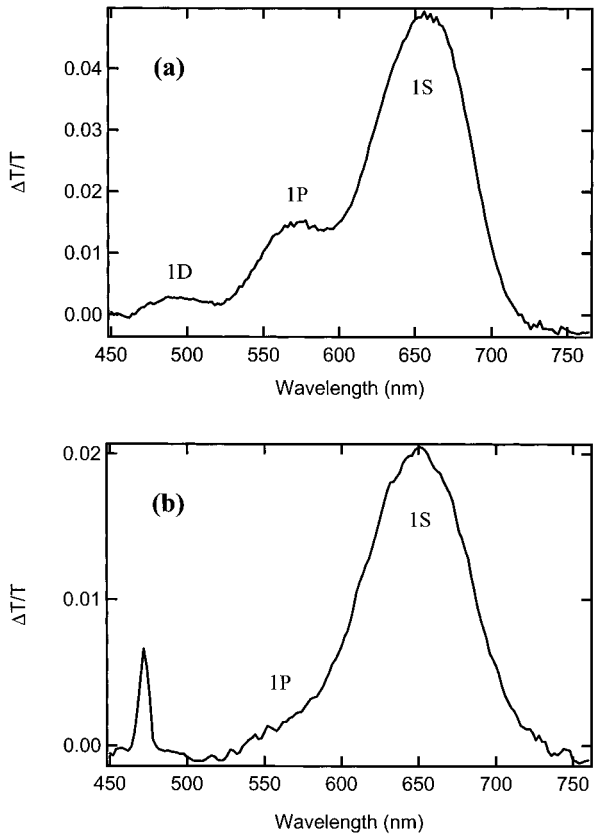

Figure 6. Transient absorption spectra for 42 Å diameter InP QDs. The structure observable in the spectrum depends on the size distribution. Narrower distributions (a) show well-defined 1P and 1D exciton transitions above the 1S, and broader size distributions (b) yield a broader transient spectrum. For (a) and (b), respectively, the excitation wavelengths were 387 and 480 nm and the time delays were 0.8 and 50 ps.

induced Stark effect and state-filling. Klimov has published spectral data for CdSe which show that the carrier-induced Stark effect produces derivative-like features in the transient absorption spectrum,[9] and we observe similar features at early times for the 1S and 1P exciton transitions following photoexcitation of InP. We observe a bleaching of higher energy (e.g., 1P) transitions which persist following charge carrier cooling; holes cooling to states lying near the VB edge may contribute to the bleaching of transitions probed by the 1P exciton energy, even in the absence of electrons occupying the $1P_e$ CB level.

Measurements of InP TA spectra on samples with sufficiently narrow size distributions indicate that up to three distinct transitions appear as significant bleaching features, starting with the 1S first exciton absorption and continuing to excitonic transitions we term 1P and 1D (see Figure 6a). These bleaching features also appear when exciting with photons insufficient to significantly populate above the $1S_e$ level. Both the carrier-induced Stark effect and state-filling can contribute to the 1P exciton bleaching; we have not yet determined their relative contributions. We do not observe a clear photoinduced absorption at long delays for energies slightly below the 1P exciton; while this may be evidence for bleaching due to hole occupation of VB levels, the size distribution of our sample prevents this conclusion. The state-filling-induced absorption change, $\Delta\alpha$, has been characterized for semiconductor QDs as a sum over excitonic transitions i, as follows:

$$\Delta\alpha(\omega) = \sum_i a_i G_i(\omega - \omega_i)(n_i^e + n_i^h) \qquad (1)$$

where $G_i(\omega - \omega_i)$ is the unit-area absorption profile of the ω_i transition, a_i is the transition area (proportional to its oscillator strength), and n_i^e and n_i^h are occupation numbers of electron and hole states involved in the transition.[9] After carriers undergo intraband relaxation, the Fermi distribution function provides the occupation numbers. Klimov has noted that, for CdSe QDs, state-filling-induced absorption changes are dominated by electrons, based on the argument that the hole populations are spread over many adjacent levels by the thermal distribution.

As a simple expression for the linear absorption based on these same excitonic transitions, the absorption can be written as

$$\alpha(\omega) = \sum_i a_i G_i(\omega - \omega_i) \qquad (2)$$

where $G_i(\omega - \omega_i)$ is again the unit-area absorption profile of the ω_i transition and a_i is proportional to the transition oscillator strength. From eqs 1 and 2, we see that the same transitions responsible for the linear absorption can, when one or both of the involved states are occupied by a charge carrier, lead to a change in absorption due to state-filling. Consider the low-carrier-density regime, such that each nanoparticle will contain at most one photoexcited electron−hole pair. As is true for CdSe QDs, in general the VB hole levels for an InP QD will be spaced more closely than the electron levels in the CB. For InP QDs with diameter $\leq$45 Å, the $1P_e-1S_e$ electron levels are spaced by $\geq$250 meV so that after relaxation to the $1S_e$ level the electron cannot thermally occupy $1P_e$. As discussed below in detail, the VB levels of an InP QD do appear to allow hole thermalization over multiple levels. Therefore, referring to eq 1, after electronic relaxation through electron−hole and hole−phonon interactions, n_i^e will have the value 1 for multiple-exciton transitions and n_i^h will have values <1 for these same transitions. The relative importance of electrons and holes to the TA signal depends principally on how strongly the thermally accessible VB levels couple to the electron level of interest. Whether electrons dominate the state-filling-induced change in absorption depends critically on the details (whether the transition is allowed, and oscillator strengths) of the excitonic transitions involving near-band-edge valence states.

We now address the issue of the contribution of electrons to the TA signal for InP QDs. Again, consider the low-carrier-density regime, such that each nanoparticle contains at most one photoexcited electron−hole pair. Electrons' domination of the TA signal relies on two assumptions: (1) that there are no additional electron levels within kT of the lowest conduction band level, so that just one state ($1S_e$) is occupied by the electron; (2) that there are several VB states spaced within energy kT available to the hole, diluting the hole contribution. Following relaxation to the $1S_e$, an electron cannot thermally occupy the $1P_e$ level near room temperature since the two lowest CB levels for a 42 Å diameter InP QD are spaced by ~270 meV, far exceeding kT at 300 K. Thus the details of the VB electronic structure determine the relative contributions of electrons and holes to the TA signal.

Theoretical electronic structure calculations for InP QDs have been made using both the **k·p** effective mass approximation method[10−12] as well as the pseudopotential approach.[13−15] Published results of **k·p** calculations of VB single particle levels show that the symmetry nature (s or p) of the first two near-band-edge states depends sensitively on the energy band parameters used for the calculation.[16,17] Independent of the energy band parameters, however, the **k·p** approach shows for a 40 Å diameter InP QD that the two lowest VB states are

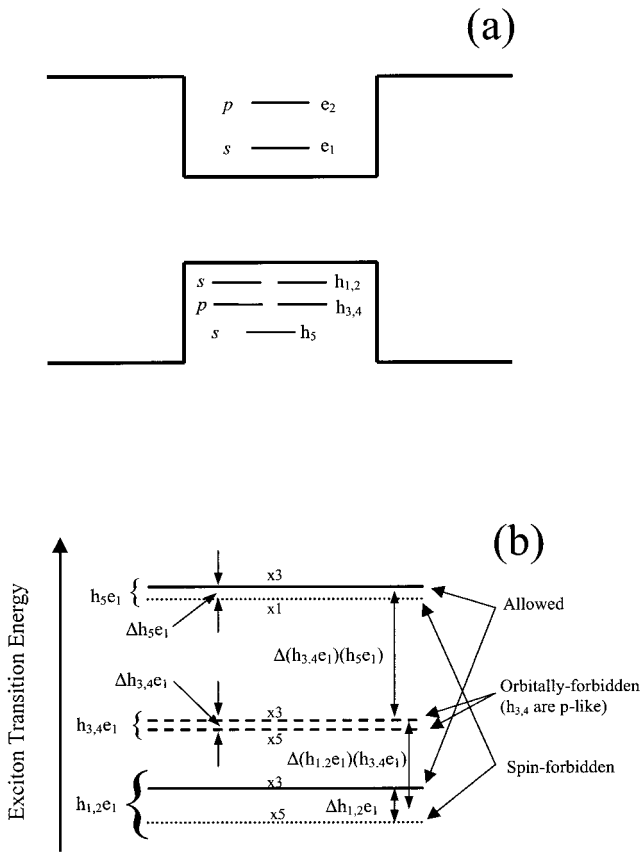

Figure 7. (a) Schematic of single-particle energy levels including the two lowest Γ-valley conduction band electron levels (e_1 and e_2) and the first five valence band hole levels (h_1-h_5). (b) Exciton transition energies for a 42 Å InP QD, including fine structure resulting from electron−hole exchange interaction. Results are based on calculations by Huaxiang Fu. Splitting values: $\Delta h_{1,2}e_1 = 5$ meV, $\Delta(h_{1,2}e_1)(h_{3,4}e_1)$ splitting = 44.5 meV, $\Delta h_{3,4}e_1$ fine structure splitting ≈ 1.5 meV, $\Delta(h_{3,4}e_1)(h_5e_1) = 66$ meV; Δh_5e_1 fine structure splitting exists but has not been calculated for this InP dot size.

spaced by ∼100 meV, or ∼4 *kT* at room temperature; therefore, this analysis shows the holes cooling to a level spaced 3−4 *kT* below the next higher VB level.

The pseudopotential approach has been used to calculate single-particle and many-particle (excitonic) energy levels and transitions for InP QDs.[13−15] Figure 7a diagrams the two lowest Γ-valley CB (L-valley single-particle levels exist between these two CB levels) and the five lowest VB single-particle levels for a 28 Å diameter InP QD.[13] Huaxiang Fu has recently calculated for the first time the single-particle levels (unpublished) for a 42 Å diameter InP QD. Single-particle levels inherently exclude electron−hole interaction effects, and therefore the hole levels $h_{1,2}$ are doubly degenerate, as are hole levels $h_{3,4}$. The dominant envelope angular momentum is given at the left side of each single particle level. H. Fu has used an atomistic pseudopotential approach[15] to calculate excitonic transitions in 42 Å InP QDs (see Figure 7b). The excitonic transitions are labeled with the single-particle levels from which they originate, with e_1, e_2 for the CB level and h_1, h_2, etc. for the VB level; these single-particle levels are the same as those presented in refs 13 and 14 for 28 and 35 Å InP QDs. Degeneracies of the excitonic transitions are listed as ×5, ×3, etc. Single-particle hole levels $h_{1,2}$ are *s*-like levels and are degenerate until the electron−hole exchange interaction splits them; the same is true for $h_{3,4}$, which are *p*-like levels. For InP QDs, the spacing between the two lowest allowed (spin and orbitally) exciton transitions remains roughly constant as a function of dot size at ∼110 meV, corresponding to the spin−orbit splitting for InP.[13] Thus, the theory shows that, while the spacing between $h_{1,2}e_1$ and $h_{3,4}e_1$ transitions decreases with increasing dot size, the spacing between $h_{3,4}e_1$ and h_5e_1 simultaneously increases. The calculations and this discussion do not include the effect of crystal field splitting, which would arise for any nonspherical dot shape (and thus likely does have an effect for "real-world" dots). Crystal field splitting would change the degeneracy of excitonic transitions involving near-band-edge hole levels. The important aspects of Figure 7b include the following:

1. The lowest excitonic transition originates from the *s*-like hole level denoted as $h_{1,2}$ (doubly degenerate until application of the "fine structure" splitting due to electron−hole exchange interaction), and involves also the *s*-like lowest energy electron level e_1. In the configuration interaction (many particle, excitonic transitions),[14,18] $h_{1,2}$ splits into two excitonic transitions involving e_1 which are separated by ∼5 meV. The lowest of these transitions is spin-forbidden, and thus nonabsorbing (and presumably also not bleached by state-filling), and is 5 times degenerate. The next higher transition is 3 times degenerate, and is allowed; therefore, we should expect that significant absorption occurs at that energy.

2. $h_{3,4}$ are (primarily) *p*-like single-particle levels, and therefore the $h_{3,4}e_1$ transitions are orbitally forbidden. The first orbitally allowed excitonic transition involving *p*-like single-particle levels would be that of $h_{3,4}e_2$. Note here that if the single-particle hole levels $h_{3,4}$ are thermally accessible to the hole, they can effectively contribute to a bleach of the "1P" transition ($h_{3,4}e_2$) without the electron occupying e_2 ($1P_e$).

3. The second allowed excitonic transition involves single-particle levels h_5 and e_1, both primarily *s*-like. The spacing between the two lowest allowed excitonic transitions is ∼110 meV.

That the pseudopotential theory predicts an exchange splitting of the lowest excitonic transition between *s*-like single particle levels is important for two reasons. First, QDs for which a single exciton occupies the lowest level (spin-forbidden and dark) will not contribute to the 1S absorption bleach, and the electron will hold the majority of the influence on the TA signal. Second, since the lowest level is dark, we should expect that for sufficiently low temperature (e.g., 10 K), we can cool the excitons completely into the dark level. The proposed low-temperature measurement allows us the opportunity to clarify agreement between theory and experiment.

The occupation probability for the various VB levels available to the hole depend on the product of the Fermi function and the density of states (or in this case, the state degeneracy). The relative (nonnormalized) hole occupation density is then

$$\rho(\epsilon_j) = f(\epsilon_j)\eta_j^{\,h} = \frac{1}{e^{-\epsilon_j/kT} + 1}\eta_j^{\,h} \qquad (3)$$

where $\eta_j^{\,h}$ is the degeneracy for the VB state *j*. Therefore, if we take the lowest single-particle hole level as the point of zero energy for the hole, energy level occupation numbers are given by eq 3. This suggests that the (lowest) spin-forbidden exciton level will very probably be occupied by an exciton. Additionally, since the hole single-particle levels associated with the $h_{3,4}e_1$ excitonic transitions are thermally accessible at room temperature, holes will also occupy the corresponding VB single-particle levels; note, however, that the $h_{3,4}e_1$ excitonic transitions are orbitally forbidden.

Our transient absorption measurements on InP QDs have yet to reveal an identifiable hole-state-specific interband transition,

so we are unable to present experimental evidence to compare with this aspect of theory. While we have not observed the ~110-meV-spaced transition, low-temperature nanosecond hole-burning measurements on 34 Å diameter InP QDs reported by Banin et al. indicate a second excited transition spaced ~100 meV from the first exciton absorption.[11] The authors note that the extracted oscillator strength for the second transition is ~1.5 times that of the lowest transition. That the two lowest excitonic transitions are spaced by ~110 meV and show comparable oscillator strength, together with the large $1S_e$–$1P_e$ spacing, suggests that the lowest energy VB hole level is primarily *s*-like. By measuring the transient absorption at 77K, the effect of hole thermalization would likely become evident and provide us with one independent measure of the presence of additional valence band states very close to the band edge.

The rate of hot charge carrier relaxation in QDs has been a topic of particular interest: the concept of the "phonon bottleneck" proposes that the large gaps between adjacent conduction[19−21] or valence[22] band levels prevents efficient carrier cooling by phonon emission. The $1S_e$ and $1P_e$ levels for 42 Å diameter InP QDs are spaced by ~270 meV, which represents an interstate gap of approximately seven LO phonon energies (40 meV). Previous research on CdSe QDs has shown that the electron−hole interaction permits an alternate, efficient cooling process. In particular, despite the inefficiency of the electron−phonon scattering mechanism for cooling, a "hot" electron can cool efficiently by an Auger-like scattering process whereby the electron transfers energy to the hole, which in turn cools efficiently through the more closely spaced states of the valence band.[23,24] Recent work has argued, based in part on the existence of a large Stokes shift of the global PL, that CdSe QDs exhibit evidence of a significant gap in the near VB edge states which slows the final cooling of the hole.[22] In contrast, previous research based on fluorescence line narrowing has shown that the large global PL Stokes shift for CdSe and InP QDs originates in the inhomogeneous particle size distribution[5,25] and reduces to the ~ <10 meV range when exciting a small range of particle sizes. This apparent contradiction presents an important question regarding the magnitude of the fine structure splitting in colloidal semiconductor QDs, the resolution of which may have important implications for excitonic relaxation dynamics in QDs.

Charge carrier relaxation studies generally assume that on an ultrafast time scale excitons either remain hot or cool to the band edge. Our data indicate the existence of an additional possible channel for energetic charge carriers. Failure of an exciton excited within a QD to contribute to band-edge bleaching and PL implies specifically that one or both charge carriers do not relax to the states contributing to these signals. At least one charge carrier either remains hot or exits the relaxation channel involving spherically symmetric QD core electronic states in favor of surface or capping molecule states. This charge carrier may either scatter into a surface-specific state or exit the particle to reside on a surface capping molecule; either process would then lead to nonradiative recombination.

For a carrier scattering or capture process to compete with intraband relaxation, the time constant should compete with that of the intraband cooling process. The rise time in 42 Å InP QDs for 1S bleaching following excitation at 3.20 eV is 280 fs. Transient absorption measurements on CdSe QDs in pyridine indicate that hole transfer to surface pyridine molecules occurs in 450 fs, providing evidence that such a carrier transfer process can indeed compete with charge carrier cooling.[24] Hole capture by a surface-bound reducing agent may show an energy dependence due to improved overlap between the energy bands of the semiconductor and the reductant. Additionally, it is not surprising that the reduced PL and band-edge TA efficiency shows a gradual onset with increasing excitation energy. Colloidal QDs are inherently inhomogeneous in exact size and shape, and their surface chemistry likely varies significantly within the aggregate sample. Such inhomogeneity produces concomitant variation in electronic and surface properties, and due to variations between dots within the sample, a sharp energy threshold for carrier "capture" by surface or capping molecule states is not expected.

Conclusion

We have shown that, for colloidal InP QDs, the excitation energy affects the efficiency with which photoexcited charge carriers relax back to states contributing to band-edge PL and photoinduced bleaching. In particular, increasing the excitation photon energy above the first exciton transition leads to reduced relaxation efficiency, suggesting that a channel develops to divert carriers from relaxing to the band-edge states. Our results suggest the ultrafast departure of one or both charge carriers from the ladder of excitonic energy levels to either surface-specific states or surface capping molecules. The PL and TA show that the "alternate" relaxation channel which is followed by higher energy excitons leads to more strongly nonradiative recombination. Further measurements are planned to distinguish whether electrons, holes, or both are diverted from relaxation through the dot excitonic levels.

Acknowledgment. The authors appreciate the assistance of Barton Smith, Gabriel Bester, Marco Califano, and Alex Zunger with very useful discussion of theory. In addition, the authors thank Huaxiang Fu for contributing the pseudopotential calculations of excitonic transitions for 42 Å InP QDs. The authors thank the US Department of Energy, Office of Science, Office of Basic Energy Sciences, Division of Chemical Sciences, for generous financial support.

References and Notes

(1) Micic, O. I.; Sprague, J. R.; Lu, Z.; Nozik, A. J. *Appl. Phys. Lett* **1996**, *68*, 3150.

(2) Hoheisel, W.; Colvin, Y. L.; Johnson, C. S.; Alivisatos, A. P. *J. Chem. Phys.* **1994**, *101*, 845.

(3) Rumbles, G.; Selmarten, D. C.; Ellingson, R. J.; Blackburn, J. L, Yu, P.; Smith, B. B.; Micic, O. I.; Nozik, A. J. *J. Photochem. Photobiol., A: Chem.* **2001**, *142*, 187.

(4) Leatherdale, C. A.; Kagan, C. R.; Morgan, N. Y.; Empedocles, S. A.; Kastner, M. A.; Bawendi, M. G. *Phys. Rev. B* **2000**, *62*, 2669.

(5) Micic, O. I.; Cheong, H. M.; Fu, H.; Zunger, A.; Sprague, J. R.; Mascarenhas, A.; Nozik, A. J. *J. Phys. Chem. B* **1997**, *101*, 4904.

(6) Klimov, V. I.; Mikhailovsky, A. A.; McBranch, D. W.; Leatherdale, C. A.; Bawendi, M. G. *Science* **2000**, *287*, 1011.

(7) Klimov, V. I.; McBranch, W. *Opt. Lett.* **1998**, *23*, 277.

(8) Poles, E.; Selmarten, D. C.; Micic, O. I.; Nozik, A. J. *Appl. Phys. Lett.* **1999**, *75*, 971.

(9) Klimov, V. I. *J. Phys. Chem. B* **2000**, *104*, 6112.

(10) Efros, A. L.; Rosen, M.; Kuno, M.; Nirmal, M.; Norris, D. J.; Bawendi, M. *Phys. Rev. B* **1996**, *54*, 4843.

(11) Banin, U.; Cerullo, G.; Guzelian, A. A.; Bardeen, C. J.; Alivisatos, A. P.; Shank, C. V. *Phys. Rev. B* **1997**, *55*, 7059.

(12) Efros, A. L.; Rosen, M. *Annu. Rev. Mater. Sci.* **2000**, *30*, 475.

(13) Fu, H.; Zunger, A. *Phys. Rev. B* **1998**, *57*, R15064.

(14) Franceschetti, A.; Fu, H.; Wang L. W.; Zunger, A. *Phys. Rev. B* **1999**, *60*, 1819.

(15) Fu, H. *Phys. Rev. B* **2002**, *65*, 45320.

(16) Efros, A. L.; Rosen, M. *Appl. Phys. Lett.* **1998**, *73*, 1155.
(17) Fu, H.; Wang, L.-W.; Zunger, A. *Appl. Phys. Lett.* **1998**, *73*, 1157.
(18) Zunger, A. *MRS Bull.* **1998**, *23*, 35.
(19) Boudreaux, D. S.; Williams, F.; Nozik, A. J. *J. Appl. Phys.* **1980**, *51*, 2158.
(20) Bockelmann, U.; Bastard, G. *Phys. Rev. B* **1990**, *42*, 8947.
(21) Benisty, H.; Sotomayor-Torres, C. M.; Weisbuch, C. *Phys. Rev. B* **1991**, *44*, 10945.
(22) Xu, S.; Mikhailovsky, A. A.; Hollingsworth, J. A.; Klimov, V. I. *Phys. Rev. B* **2002**, *65*, 045319.
(23) Guyot-Sionnest, P.; Shim, M.; Matranga, C.; Hines, M. *Phys. Rev. B* **1999**, *60*, R2181.
(24) Klimov, V. I.; Mikhailovsky, A. A.; McBranch, D. W.; Leatherdale, C. A.; Bawendi, M. G. *Phys. Rev. B* **2000**, *61*, R13349.
(25) Norris, D. J.; Efros, A. L.; Rosen, M.; Bawendi, M. G. *Phys. Rev. B* **1996**, *53*, 16347.